Vol. 749: 57–69, 2024
https://doi.org/10.3354/meps14727

MARINE ECOLOGY PROGRESS SERIES
Mar Ecol Prog Ser

Published November 21

Nutrient enrichment can increase the thermal performance of Galápagos seaweeds

Haley E. Capone[1,*], Margarita Brandt[2,3], Paul W. Gabrielson[1], John F. Bruno[1,3]

[1]Department of Biology, The University of North Carolina at Chapel Hill, Chapel Hill, NC 27599-3280, USA
[2]Colegio de Ciencias Biológicas y Ambientales COCIBA, Universidad San Francisco de Quito (USFQ), Quito 170901, Ecuador
[3]Galapagos Science Center (GSC), Universidad San Francisco de Quito (USFQ) and University of North Carolina at Chapel Hill (UNC), Avenida Alsacio Northia S/N, Puerto Baquerizo Moreno 200101, Ecuador

---

ABSTRACT: Thermal sensitivity in ectothermic organisms is often contingent upon environmental factors. Nutrient availability in particular is believed to influence the physiological responses of primary producers to global warming and is thus relevant to consider when forecasting the structure and functioning of future marine ecosystems. This study measured the effect of nutrient enrichment on the thermal sensitivity of 4 genera of Galápagos seaweeds (*Ulva*, *Caulerpa*, *Padina*, and *Ochtodes*), estimated as the thermal optimum (T_{opt}), performance maximum (P_{max}), activation energy, and deactivation energy. These parameters were quantified by modeling thermal performance curves for net photosynthesis under ambient and nutrient-enriched conditions. Our findings revealed variation in T_{opt} among genera, ranging from 27.6° to 36.0°C. Nutrient additions enhanced T_{opt} by ~2°C for 2 (*Padina* and *Caulerpa*) of the 4 taxa and also significantly increased P_{max} in *Padina*, suggesting the ability for warming-induced ocean stratification and associated effects (i.e. decreasing nutrient availability) to reduce the capacities of these populations to maintain and support new growth. No significant differences in T_{opt} or P_{max} were observed for either *Ulva* or *Ochtodes* with enrichment. Ambient net photosynthesis and respiration rates were also compared across genera; P_{max} rates for net photosynthesis were consistently higher than those for respiration (i.e. until just beyond T_{opt}); however, photosynthetic T_{opt} values were lower. Thus, this study suggests that further warming could reduce overall net primary productivity, with potentially far-reaching implications for marine food webs.

KEY WORDS: Physiology · Thermal tolerance · Marine macroalgae · Climate change · Marine ecology

1. INTRODUCTION

Recent work has highlighted the importance of local environmental conditions in mediating the thermal tolerance of marine organisms in the context of global warming (Wolff et al. 2018, França et al. 2020, Gissi et al. 2021). Variables such as salinity, CO_2, irradiance, and nutrient levels are all believed to influence an individual's thermal sensitivity (Drohan et al. 2005, Elser et al. 2007, Russell et al. 2009, Takolander et al. 2017). Nutrient availability is an especially significant factor for the ocean's primary producers, influencing metabolic maintenance and interacting with temperature to shape primary production and food web dynamics (Elser et al. 2007, Litchman & Thomas 2023).

Contemporary investigations have documented the effects of nutrients on the thermal tolerance of primary producers across aquatic ecosystems. In lake environments, increasing phosphate — a typically limited nutrient — can raise the thermal optima of freshwater phytoplankton by up to 15°C (Bestion et al. 2018). Some temperate marine species show positive effects of nitrate; for example, the growth and photosynthetic rates of *Fucus vesiculosus* and *Macrocystis*

---

*Corresponding author: hecapone@gmail.com *pyrifera* increase with nitrate enrichment at elevated temperatures (≥18° and ≥14°C, respectively) (Colvard & Helmuth 2017, Fernández et al. 2020), whereas other studies have found no effect of nitrate additions on growth (Mabin et al. 2013) or survival (Weigel et al. 2023) at high temperatures.

Beneficial effects of nutrients on thermal sensitivity may arise from various potential underlying mechanisms. Nitrogen plays a crucial role in regulating enzymatic activities and productivity (Fernández et al. 2020); its limitation, as seen in *Saccharina latissima*, has been linked to the suppression of heat shock protein production and impairment of the photosynthetic apparatus (i.e. a decline in RuBisCO activity and the density of photosystem II reaction centers) (Gerard 1997), both essential for plant stress tolerance at high temperatures. Additionally, antioxidants like carotenoids, vital for maintaining algal photosynthetic rates and reducing reactive oxygen species under heat stress, are most effective under nutrient-replete conditions (Eismann et al. 2020).

The potential for nutrients to mitigate the adverse effects of warming on thermal tolerance has recently been formalized mathematically by combining a thermal performance curve (TPC) with the saturating dependence of growth on nutrient concentration, known as the Monod equation (Thomas et al. 2017). Integrating these 2 functions results in an 'interactive double-exponential' model describing the combined effects of temperature and nutrient concentration on physiological performance (Thomas et al. 2017, Bestion et al. 2018). This theoretical framework enables the prediction of thermal performance parameters under the interactive influence of temperature and nutrient availability, providing insights into an organism's physiological state. According to the theory, as nutrient concentrations increase, the performance maximum (P_{max}) — representing an organism's peak performance rate — is predicted to rise along with the thermal optimum (T_{opt}). These increases suggest the maintenance of physiological performance despite warmer and unfavorable ambient conditions, as illustrated in Fig. 1.

Understanding species' physiological responses in the context of combined local and global environmental stressors, including climate warming, is necessary for practical conservation efforts. One important aspect of anthropogenic climate change is increasing stratification in the ocean, which impedes the upward movement of nutrients from deeper water layers to the mixed surface layer, leading to a reduction in available nutrients (Li et al. 2020, Van De Waal & Litchman 2020). In addition, nutrient trapping can enhance the movement of nutrients to the deep ocean, strengthening this limitation (Van De Waal & Litchman 2020). These pronounced changes in vertical mixing dynamics could adversely affect primary producers if they experience reductions in water column nutrients and tissue nutrient reserves, compromising their ability to derive associated metabolic benefits and thereby limiting overall marine ecosystem productivity (Laufkötter et al. 2015, Fu et al. 2016).

In the rocky shallow subtidal (1–3 m depths) of the Galápagos archipelago, seaweeds play a dominant role in the benthic community, providing a critical habitat structure and nutritional source for a diverse herbivore assemblage (Edgar et al. 2010, Carr et al. 2018). As temperature and nutrient fluxes in the Galápagos vary significantly with the El Niño–Southern Oscillation cycle — and across seasons and locations due to the complex patterns of large-scale currents and local upwellings (Schaeffer et al. 2008) — it is critical to understand how warming-induced changes in environmental conditions (i.e. declining nutrient availability) may influence the physiological responses of primary producers. Elucidating the interplay of these factors on thermal performance would not only allow us to predict future patterns of seaweed distribution and abundance, but also help us

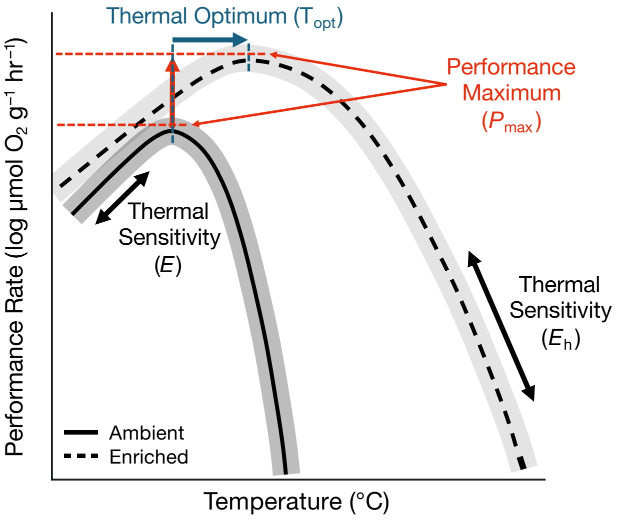

Fig. 1. Thermal performance curve with associated thermal performance parameters under low and high nutrient availability. The dashed curve represents the predicted response of an alga residing in a nutrient-enriched environment, where peak physiological performance (P_{max}) and the thermal optima (T_{opt}) are higher than those for an alga under ambient conditions (solid line). Note the thermal sensitivities (slope activation and deactivation energies, E and E_h, respectively), which may be less steep at elevated nutrient levels, suggesting reduced sensitivity to higher temperatures with enrichment

understand broader ecosystem dynamics (Thomson et al. 2015, Thomas et al. 2017, Detmer et al. 2021).

Our study investigated the effect of nutrient enrichment on the thermal sensitivity of marine seaweeds, and hence their primary production, explicitly testing the hypothesis that nutrient enrichment would increase photosynthetic T_{opt} and $P_{\max}$ (Fig. 1). We used 4 common subtidal seaweed genera in the Galápagos Archipelago: *Ulva*, *Caulerpa*, *Padina*, and *Ochtodes*. Theory suggests that higher nutrient concentrations may enhance T_{opt} and $P_{\max}$ as well as the shape and breadth of TPCs, which we characterized as activation (E) and deactivation (E_{h}) energy slopes. Specifically, we hypothesized that nutrient enrichment would reduce the energy slopes for photosynthesis, decreasing sensitivity to warming.

2. MATERIALS AND METHODS

2.1. Study system and seaweed collections

This study's field and experimental procedures occurred at and around the Galapagos Science Center (GSC) on San Cristóbal Island in the eastern Galápagos Archipelago. In June 2022, we conducted thermal performance experiments on seaweeds from 4 genera of the 3 marine macroalgal groups — Chlorophyta (*Ulva* and *Caulerpa*), Phaeophyceae (*Padina*), and Rhodophyta (*Ochtodes*). We collected genera from 3 shallow subtidal areas — Playa Mann, Punta Carola, and Bahía Rosa Blanca — where established populations of each were apparent and suitable for multiple-replicate sampling. For more detailed information regarding sampling sites and genus-specific characteristics, see Table S1 in the Supplement at www.int-res.com/articles/suppl/m749p057_supp.pdf and Capone (2023).

2.2. DNA sequencing for algal identification

To unambiguously identify seaweed species (Gabrielson et al. 2024), dried algal thalli from each genus across 4 treatment conditions (see Section 2.3) were randomly selected and shipped in plastic vials containing desiccant beads from the GSC to the University of North Carolina at Chapel Hill for DNA sequencing. Total cellular DNA was extracted from each algal thallus (except *Padina*, for which amplifiable DNA extraction failed) following the method in Hughey et al. (2001); the PCR amplification protocol was also from Hughey et al. (2001). The plastid-encoded *tuf*A gene was amplified from the green algal genera *Ulva* and *Caulerpa* using the primer set GazG4/GazAR (Saunders & Kucera 2010). The plastid-encoded *rbc*L gene was amplified from the red algal genus *Ochtodes* using the primer set F753/RrbcS (Freshwater & Rueness 1994). PCR products were cleaned with the Qiagen PCR Purification Kit, cycle-sequenced, and sent to the DNA Analysis Core Facility at the Marine Sciences Center, University of North Carolina, Wilmington, for Sanger sequencing. Sequences were manually aligned and compiled using Sequencher v.5.4.6 (Gene Codes Corporation). The Basic Local Alignment Search Tool (BLAST) on the National Center for Biotechnology Information website was used to identify *Ulva* and *Caulerpa* specimens to species (> 99% sequence identity).

BLAST results of DNA sequences obtained from experimental specimens revealed one species of *Caulerpa*, *Caulerpa racemosa* (hereafter *Caulerpa*), 2 species of *Ulva* (*U. ohnoi* and *U. lactuca*), and at least 2 species of *Ochtodes* (Table A1 in the Appendix). One is likely *O. crockeri*, with a type locality in the Galápagos Archipelago. However, the type specimen has not been sequenced, and the application of the name to specimens we sequenced is uncertain. Most macroalgal species are cryptogenic and exhibit habitat overlap; therefore, determining specific thalli to species level before an experiment is often impractical. Consequently, seaweeds are rarely sequenced before experimentation and are typically chosen based on field observations of gross morphology (e.g. Wernberg et al. 2016, Bennett et al. 2022). Our study was designed to measure the thermal sensitivity of primary producers at the genus level, except for *Caulerpa*, where all sequenced samples were *C. racemosa*.

2.3. Acute thermal stress experiment to measure sensitivity

The experiment was fully factorial in its design, crossing nutrient availability (ambient and nutrient-enriched conditions) with temperature. Two measures of metabolism (net photosynthesis and respiration) were quantified under both nutrient availabilities and ramped across 12 sequential temperatures (16°, 20°, 22°, 24°, 26°, 28°, 30°, 32°, 34°, 36°, 39°, and 42°C). In the context of our study, the 'ambient' condition consisted of water that was sourced from the sea (~100 m from the marine laboratory), stored in two 2000 l tanks, and processed through a high-quality filtration system (RainHarvest Systems Triple 20 Inch Big Blue

Filter Assembly, Blue, L-R, 20 µm pleated sediment filter, a 5 µm pleated sediment filter, and a 1 µm activated carbon block filter; SKU 17695) to minimize plankton and microbial activity during performance trials. We assumed that the concentration of nutrients in ambient seawater was limiting to photosynthesis, as is typical for shallow tropical seas (Fong et al. 2003, Littler et al. 2006).

For the nutrient-enriched treatment, we experimentally increased nitrogen levels to ~140 µmol l^{-1}, 10 times higher than those reported in coastal regions of San Cristóbal Island (Schaeffer et al. 2008), i.e. to concentrations above those limiting to productivity. Similarly, phosphorus concentrations were elevated ~22-fold. Note that nutrients were intentionally added in levels higher than natural conditions but kept below concentrations at which they would become toxic. The goal of the enrichment was not to replicate field conditions but to instead alleviate nutrient limitations. Each evening preceding a nutrient trial day, we prepared the enriched treatment by dissolving 0.78 g l^{-1} of a soluble nitrogenous fertilizer (Grow More Inc.; Vitafol 30-10-10 NPK; Ecuafol) in a measured amount of filtered ambient seawater from a 120 l shallow bin. The solution was then warmed to ensure complete dissolution and added back to the bin, where it was allowed to mix overnight with the aid of air stones (Marina 1-inch Cylinder Air Stone, model A962).

Thermal performance trials were conducted daily at the GSC from 11–28 June 2022. During this period, La Niña was active in the eastern Pacific (Ormaza-González 2023). Ambient sea surface temperatures were recorded near collection sites on San Cristо́bal Island (cool season min.: 14.6°C on 28 October 2022; max.: 25.1°C on 9 June 2022; mean during trials: 20.2°C; Cerro Mundo HOBO logger), and average ambient temperature during the trial period was included in TPC model-fitting (see Section 2.5). Before each trial, we collected 9 replicate thalli of a given genus, spaced at least 5 m apart, resulting in 36 experimental fragments per genus (9 per treatment combination). After collection, thalli were promptly transported in seawater to the laboratory, where they were weighed to ensure uniform size and weight (±2 g), reducing the potential for self-shading and mass-dependent temperature effects, respectively (Nejrup et al. 2013, Best et al. 2015, Speare et al. 2022). Thalli were then placed inside a bin containing ambient seawater and allowed to heal and acclimate to the laboratory environment for ~1 h while respirometry equipment was arranged for the first temperature incubation. Temperature regulation (±0.3°C) was achieved using a thermostat control system (Inkbird ITC-308 Digital Temperature Controller 2-Stage Outlet Thermostat Heating and Cooling) along with 2 bucket heaters (Kingwork Bucket Heater Model 05-742G 1000 W, Gesail Immersion Heater Model HST-WH1111 1500 W) and chillers (AquaEuroUSA Max Chill-1/13 HP Chiller). Filtered seawater was chilled to 16°C nightly before a trial, both in the 120 l bin and a 142 l cooler (Quick and Cool 150 Qt Cooler, item no. 00044363), which housed a custom-made closed respirometry system (Australian Institute of Marine Science). Thalli were randomly allocated to 1 of 9 acrylic respirometry chambers (680 ml each), secured into their respective slots on the respirometry table, and placed beneath a black, non-transparent tarp to block all light (see Fig. S1a in the Supplement). If it was a light trial day (i.e. measuring net photosynthesis), a full-spectrum aquarium light (MARS AQUA 300 W LED) suspended above respiratory chambers was set to a mean (±SE) light level of 315 ± 15 µmol photons m^{-2} s^{-1} (from photosynthesis–irradiance [*P*–*I*] pilot light trials; see Section 2.4). Before the start of a light trial temperature incubation, the light level was measured for each chamber position on the respirometry table using an underwater cosine-corrected sensor (Apogee MQ-510 Full-Spectrum Underwater Quantum Light Meter, spectral range: 389–692 [±5] nm) to ensure that there was relative consistency of irradiance across chambers.

Oxygen evolution inside each chamber was quantified using a PreSens Oxygen Meter System (OXY-10 SMA [G2]) with fiber-optic oxygen probes (PreSens dipping probes [DP-PSt7-10-L2.5-ST10-YOP]) and temperature probes (Pt1000) (Fig. S1a). Oxygen concentration measurements were recorded using PreSens Measurement Studio 2 software (v.3.0.3.1703) at 1 s intervals throughout a given temperature incubation, typically lasting 15 min. Note that this duration was determined based on the time needed to estimate a constant metabolic rate (log[µmol O_2 g^{-1} h^{-1}]), and the elicited responses reflect methods used to measure instantaneous stress (commonly employed in many field fresh studies; e.g. Silbiger et al. 2019, Silva-Romero et al. 2021) that have recently been corroborated by longer-term *in situ* experiments (Morikawa & Palumbi 2019, Voolstra et al. 2020). Thus, measured algal responses may reflect higher thermal sensitivity than would otherwise occur in a natural setting, and results should be interpreted with this caveat (i.e. limited acclimatization potential) in mind.

Each chamber was equipped with a magnetic stir bar that, when locked into the motor-powered stirring table (Fig. S1a), rotated at 200 rpm to ensure continuous water circulation and prevent oxygen supersaturation, following the procedure described by Silbiger et al. (2019). To adjust for background metabolic activity from microorganisms and bacteria in the seawater (although rates were minimal due to the use of filtered seawater), we randomly chose one empty chamber to act as a control for each treatment combination for each genus (see Fig. S1b), using its oxygen evolution as the baseline rate. This rate was then subtracted from the readings of treatment chambers, isolating oxygen evolution to seaweeds only. Any measurement abnormalities (i.e. an oxygen bubble contacting the fiber-optic probe falsely spiking oxygen readings) were documented and later removed from the data files before analysis.

Between each temperature incubation, water was heated with bucket heaters inside the bin and cooler simultaneously, and air stones oxygenated water inside the bin to saturation. After a 10–20 min warming period (during which algae were held at the previous incubation's temperature to help standardize potential acclimation effects), both reservoirs reached a constant, uniform temperature, and the chambers were replenished with newly warmed and circulated seawater from the heated bin. This process aimed to reset O_2 and CO_2 levels while ensuring their concordance with the subsequent temperature of the cooler. The bin contained either ambient or enriched seawater, depending on the trial day. Water was not reused between temperature incubations, and no additional water was added mid-trial to maintain consistent nutrient levels across all incubations. Additionally, chillers were labeled and assigned the same treatment condition across all experimental trials to avoid cross-treatment contamination.

At the end of the final temperature incubation on a given trial day, water volume displacement was measured for each chamber and used to estimate the amount of water inside the chamber to standardize oxygen concentration measurements. Excess water from the algae was then removed using a salad spinner (10 spins each) before recording wet biomass for each thallus. Subsequently, thalli were desiccated in a drying oven (Memmert UFE 400 Sterilizer Laboratory Oven) at 60°C for 24 h, following the method described for sea urchins by Silva-Romero et al. (2021). After drying, each thallus was reweighed to determine the dried organic tissue mass, subtracted from its respective wet mass to normalize the metabolic rate by the amount of dehydrated, organic tissue, following Larsson et al. (2013).

2.4. Estimation of saturating irradiance

To ensure net photosynthesis rates were recorded at a light level capturing optimal photosynthetic efficiency across seaweed taxa, Photon Flux Density (PFD) was measured at one of our collection sites using a light sensor logger (LI-COR LI-1500 Quantum Sensor) to quantify the natural light regime. Daily peak irradiance under varying cloud cover conditions was measured at a depth of 1 m on 5 different days, resulting in daily means of 309, 215, 368, 338, and 421 µmol photons m^{-2} s^{-1} (overall mean: 330 ± 34 µmol photons m^{-2} s^{-1}). Photosynthesis–PFD curves, or P–I curves, were developed using samples from 3 of the 4 genera (n = 6; 2 thalli per genus) to determine saturating irradiance (I_k) levels for experimental trials. *Caulerpa* was excluded from these measurements due to its distance from the GSC and limited sampling capabilities. However, previous work on this genus suggests a favorable range of light intensity between 88 and 338 µmol photons m^{-2} s^{-1} (Komatsu et al. 1997), which includes our selected light level for net photosynthesis trials in the study. Oxygen production within all chambers was measured during a 20 min incubation period at a constant ambient temperature of 22°C under 10 sequential PFDs (0, 52, 88, 132, 212, 280, 364, 432, 551, and 577 µmol photons m^{-2} s^{-1}). The light level for every chamber was quantified before each sequential PFD incubation to ensure uniformity. The PFD series created a P–I curve fit to identify I_k and the photoinhibition point for all genera (Fig. S2 in the Supplement). Specifically, a nonlinear least squares regression (Marshall & Biscoe 1980) of a non-rectangular hyperbola was employed to calculate the P–I curve parameters based on the model equation described in Silbiger et al. (2019). Area-based net photosynthesis was measured across all net photosynthesis trials at a P–I curve-derived light level of 315 ± 15 µmol photons m^{-2} s^{-1} to reflect a value below the point of photoinhibition and above an I_k of 206 µmol photons m^{-2} s^{-1} (Fig. S2).

2.5. Statistical analysis

The PreSens oxygen evolution measurements collected for each algal thallus during a given temperature trial were used to calculate the metabolic slope for that individual's temperature incubation. This rate is then displayed as a single data point (i.e. of 9 total replicates) at each incubation, forming the basis for a TPC across the temperature ramp. These rates were quantified using repeated local linear regressions from the package 'LoLinR' (Olito et al. 2017) in R (R Core Team 2022). Specifically, 'LoLinR' utilizes a bootstrapping technique to calculate a rate based on point density, and we employed parameters for linearity (L_{pc}, sum of percentile ranks of Z_{min} scores for each element) and an α of 0.5 (proportion of total observations in the data set) for observations, thinning data by every 15 s (Olito et al. 2017). Once rates were obtained, a series of mathematical corrections were performed to account for algal chamber water volume displacement, background metabolic rates of control chambers, and algal dry weight (Silva-Romero et al. 2021). Organic-biomass-normalized rates for net photosynthesis and respiration were then log transformed (following Silbiger et al. 2019, Silva-Romero et al. 2021), preceding their fit to a modified Sharpe-Schoolfield equation for high-temperature inactivation through a nonlinear least squares regression (see Table 1 in Silbiger et al. 2019). The fits were determined using the 'nls.multsart' R package (Schoolfield et al. 1981, Padfield et al. 2017, Padfield & Matheson 2018). This function allows each parameter to begin with multiple starting values (which are randomly selected from a uniform distribution), and model selection is performed using Akaike's information criterion (AIC) to determine the best-fitting parameter set (Padfield et al. 2016). Once model fits were obtained, 95% confidence intervals (CIs) were used to estimate thermal performance parameters for a given genus and treatment. Four parameters were estimated as measures of thermal sensitivity: T_{opt}, P_{max}, E, and E_h. Specifically, we predicted that nutrient enrichment would increase T_{opt} and P_{max} while decreasing E and E_h (i.e. less steep slopes indicate reduced thermal sensitivity, as shown in Fig. 1). T_{opt} and P_{max} were obtained from the previously computed TPC parameters using the T_{opt} equation (see Table 1 in Silbiger et al. 2019).

After obtaining parameter estimations, the distribution of values for each parameter was assessed visually using histograms and quantile–quantile plots, respective to each genus × treatment combination. The interquartile range (IQR) method substituting the median and IQR for mean and standard deviation (SD) was used to identify and remove outliers from each combination because, unlike the SD approach, this non-parametric analog produces relatively robust key statistics and is resilient to assumptions of symmetry (unlike median absolute deviation) and insensitive to smaller sample sizes (Rousseeuw & Croux 1993, Leys et al. 2013, Jones 2019). Linear models were fitted using the 'lme4' package (Bates et al. preprint https://doi.org/10.48550/arXiv.1506.04967) to test the hypothesis that nutrient enrichment increases thermal tolerance. These models included the treatment (ambient versus enriched conditions) and genus as fixed effects, along with a genus × treatment interaction term. Four statistical models were created, each for one of the 4 TPC parameters. Selection using AIC and Bayesian information criterion model comparisons were performed to assess the goodness of fit of these parameter models. We assessed ANOVA assumptions of homogeneity and normality using Levene's and Shapiro-Wilk's tests, respectively. Bar plots displaying the mean (±95% CIs) response across genera for each thermal parameter were created with respect to treatment condition.

As previously implied, TPCs were also constructed from model-derived predictions of log net photosynthesis and respiration rates for the 4 genera under ambient and enriched conditions. Although trials were conducted for the respiration-enrichment combination, thermal performance parameters could not be reliably estimated from TPCs for *Ulva* spp. and *Caulerpa* due to their T_{opt} values exceeding the study temperature limit of 42°C. Consequently, TPCs (and respective statistical testing on the thermal parameters) were only modeled for the ambient-respiration combination. Therefore, any comparisons between net photosynthesis and respiration rates involve data from their respective ambient treatments, for which parameters could be confidently estimated for all taxa. All data analyses were performed in R v.4.2.2, and the source data and scripts are publicly accessible on GitHub (https://github.com/hecapone/Thermal_performance_of_Galapagos_seaweeds_under_enrichment).

3. RESULTS

Both net photosynthesis and respiration rates increased with temperature across all genera until respective T_{opt} values were reached (Fig. 2 & Fig. S3 in the Supplement). Net photosynthetic rates were consistently higher than those for respiration by at least 2 log µmol O_2 g^{-1} h^{-1} at any given temperature (Fig. 3b & Fig. S4b for mean maximum rates) until just beyond the T_{opt}, when net photosynthesis rapidly declined towards 0 log µmol O_2 g^{-1} h^{-1}, and respiration remained above 2 log µmol O_2 g^{-1} h^{-1} beyond 42°C (Fig. 2 & Fig. S3). We found significant effects of enrichment across all linear regression models of net photosynthesis for the 4 thermal performance parameters (T_{opt}, P_{max}, E, and E_h) (Table 1). Overall, enrichment significantly influenced T_{opt}, E, and E_h. In contrast, P_{max} was not affected by nutrient addition

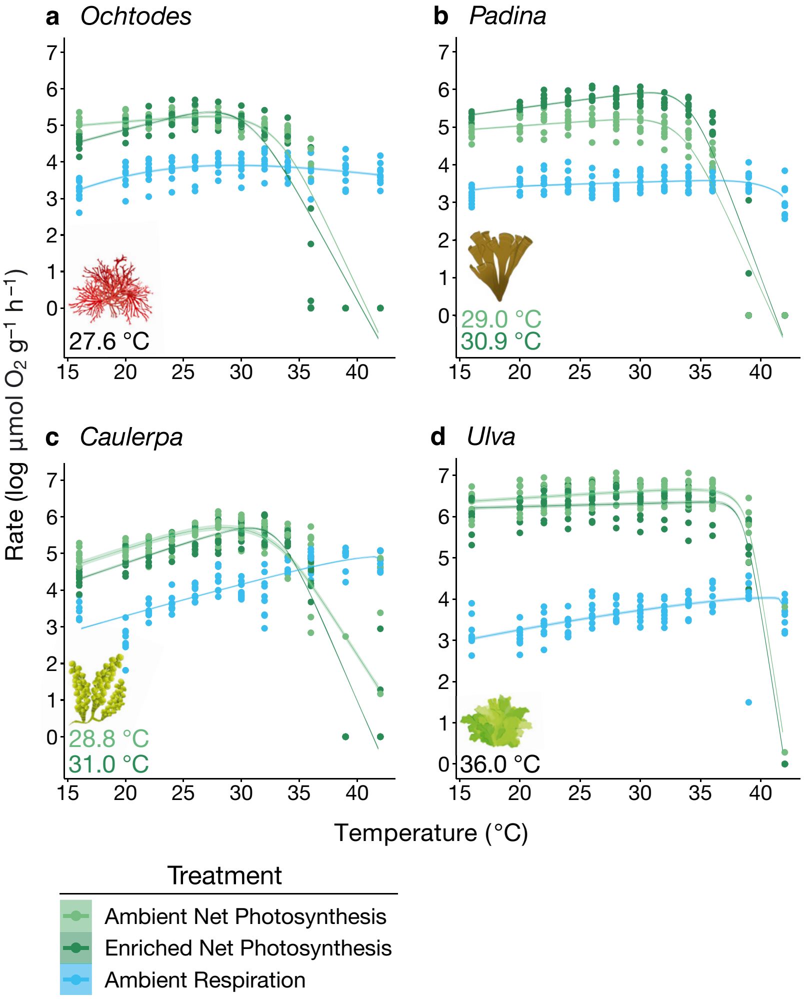

Fig. 2. Sharpe-Schoolfield-derived thermal performance curves (TPCs) of log net photosynthesis and respiration rates plotted as average model-fitted regression and 95% confidence intervals per treatment by genus. Each point represents an independent data measurement from 16° to 42°C. Plots displaying a single thermal optimum (T_{opt}, bottom-left corner) do not significantly differ in algal response to enrichment. T_{opt} values for enriched respiration exceeded the study temperature limit of 42°C for 2 of the 4 taxa, so the model could not accurately estimate the resulting regression for this treatment combination. Thus, they were omitted from display within this model-derived TPC figure

(Table 2). However, the relative magnitudes and significance of these parameters differed across genera and with treatment conditions (Figs. 2 & 3).

Net photosynthetic parameters T_{opt} and P_{max} were highest in *Ulva* (36.0°C and 6.5 log µmol O_2 g^{-1} h^{-1}, respectively) and lowest for *Ochtodes* (27.6°C and 5.3 log µmol O_2 g^{-1} h^{-1}, respectively) regardless of treatment, and neither was significantly affected by enrichment for either genus (Figs. 2a,d & 3a,b). In contrast, T_{opt} for *Padina* and *Caulerpa* and P_{max} for *Padina* were both affected by the nutrient treatment; mean T_{opt} significantly increased from 28.8° to 31.0°C in *Caulerpa* and from 29.0° to 30.9°C for *Padina* with nutrient enrichment (Figs. 2b,c & 3a). Mean P_{max} was also significantly higher for *Padina* with nutrient enrichment (5.9 log µmol O_2 g^{-1} h^{-1}) than under ambient conditions (5.2 log µmol O_2 g^{-1} h^{-1}; Fig. 3b).

The *E* parameter was significant for *Ochtodes* and *Ulva*, but effects of enrichment were different; mean *E* was lower with enrichment (0.05 eV) for *Ulva* compared to ambient conditions (0.1 eV) (Fig. 3c). In contrast, mean *E* was higher under nutrient additions (0.7 eV) than with ambient conditions (0.2 eV) for *Ochtodes* (Fig. 3c). Effects of enrichment on E_h were only significant for *Caulerpa*, in which enrichment increased average E_h to 7.3 eV (Fig. 3d). Lastly, mean E_h values were greater across all taxa than respective *E* means, regardless of treatment (Fig. 3c,d).

4. DISCUSSION

For 2 of the 4 experimental seaweeds, nutrient enrichment decreased the thermal sensitivity of net photosynthesis. Specifically, nutrient additions significantly increased the photosynthetic T_{opt} of *Padina* and *Caulerpa* and P_{max} in *Padina*. Enrichment also caused a slight, yet significant, decrease in *E* for *Ulva*. In contrast, nutrient additions did not significantly affect T_{opt} or P_{max} for *Ochtodes* or *Ulva* and, perhaps unexpectedly, increased *E* in *Ochtodes* and E_h in *Caulerpa*. These findings indicate genus-specific effects of nutrient enrichment on the thermal performance of Galápagos seaweeds. Additionally, our results may imply that ambient nutrient concentrations are limiting for taxa experiencing enhanced thermal performance under enriched conditions.

There is widespread evidence that the growth and photosynthetic efficiency of some marine primary producers are nutrient-limited (Littler et al. 1991, Pedersen & Borum 1996, Fong et al. 2003, Vermeij et al. 2010). While we did not explicitly measure growth, we observed evidence of *in situ* limitation in *Padina* and *Caulerpa*, as both showed a significant shift of photosynthetic T_{opt} toward warmer

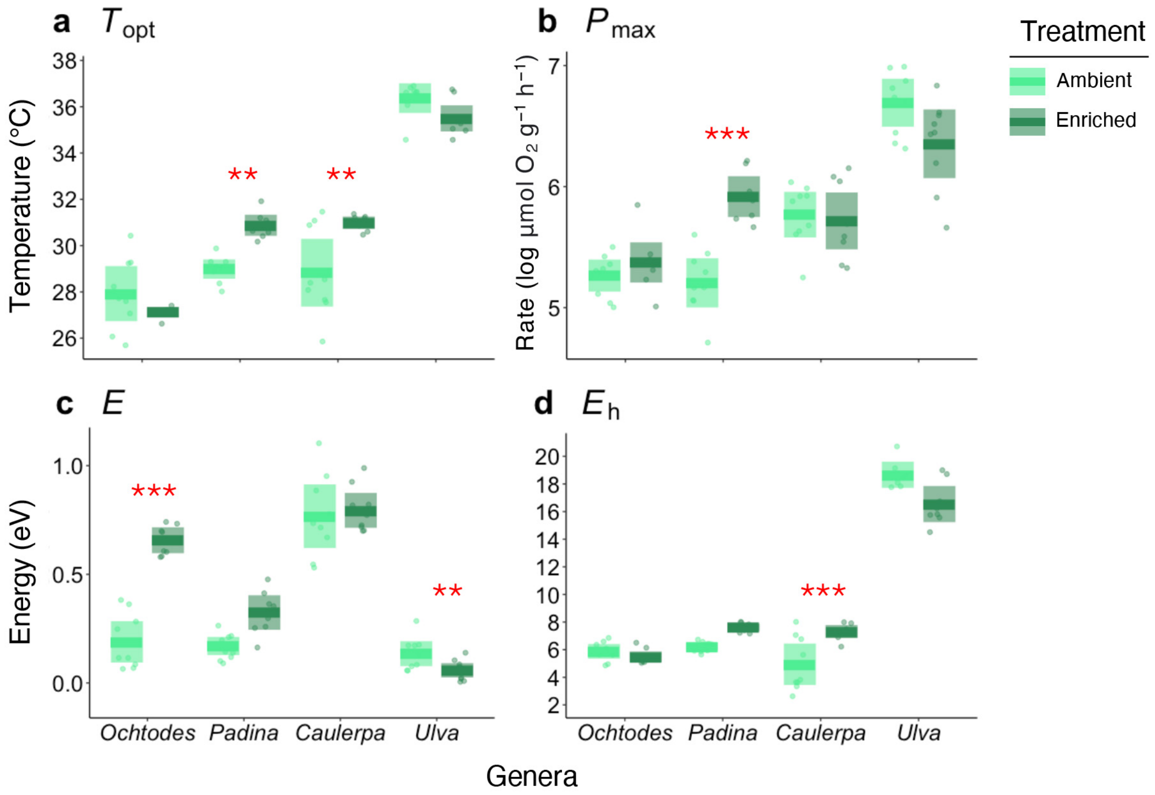

Fig. 3. Thermal performance parameters (see Fig. 1) for net photosynthesis showing measurement points by treatment (ambient versus enriched) for all individuals. Darker horizontal bands across genera: mean response for each treatment; surrounding vertical shaded regions: 95% confidence intervals. $^{**}p < 0.01$; $^{***}p < 0.001$

temperatures with enrichment. As T_{opt} represents the temperature of optimal performance for a given biological rate (i.e. growth, photosynthesis), it is a saturating function of nutrient availability (i.e. T_{opt} rises more rapidly at lower nutrient levels and decelerates as it approaches saturating concentrations) (Thomas et al. 2017, Bestion et al. 2018). Therefore, a significantly higher T_{opt} under enriched conditions suggests that these taxa are currently living below their saturation thresholds within their respective environments and may be at greater susceptibility to thermal stress induced by rising sea surface temperatures, particularly with increased stratification.

Shifting nutrient availability with ocean warming will likely differentially influence the distribution and abundance of these primary producers throughout the Archipelago. For *Padina*, we might expect a more uniform reduction in productivity when temperatures exceed 29.0°C (Figs. 2b & 3a) due to the strong physiological response of this genus to external nutrient additions (Fong et al. 2003). If ambient nutrient concentrations decline, it may be obligated to rely on its smaller internal nutrient storage to satisfy nutritional needs during heatwaves (Clausing & Fong 2016),

Table 1. Summary statistics for linear regression models, including genus × treatment interaction terms for all net photosynthesis thermal performance parameters. T_{opt}: thermal optimum; P_{max}: performance maximum; E: activation energy; E_h: deactivation energy. $^{***}p < 0.001$

Performance parameter	Resid. df	Adjusted R^2	F	p
T_{opt}	59	0.9064	92.36	***
P_{max}	63	0.7806	36.59	***
E	62	0.7879	37.61	***
E_h	59	0.8905	77.68	***

Table 2. ANOVA model summary (p-values) for net photosynthesis thermal parameters. T_{opt}: thermal optimum; P_{max}: performance maximum; E: activation energy; E_h: deactivation energy. $^{*}p < 0.05$; $^{***}p < 0.001$

Model factor	T_{opt}	P_{max}	E	E_h
Enrichment	***	9.42×10^{-2}	$4.13 \times 10^{-2*}$	***
Genus	***	***	***	***
Enrichment × genus	***	***	***	***

reducing its capacity to maintain and support new growth. On the other hand, despite uncovering similar evidence of nutrient limitation in *Caulerpa*, studies conducted *in situ* often show an absence of limitation in *Caulerpa* spp., even within low-nutrient habitats (Delgado et al. 1996, Ceccherelli & Sechi 2002). This finding is in contrast to their known high nitrogen requirements but is thought to be due to elevated nutrient-uptake capacity from the sediment using rhizoids, shown at times to account for the total nitrogen requirement (Williams 1984, Williams et al. 1985, Chisholm et al. 1996). As this genus has been documented at its highest reported densities overgrowing coral reefs in the northern islands of the Galápagos Archipelago (Glynn et al. 2018, Riegl et al. 2019, Keith et al. 2022), such findings may suggest that *Caulerpa* is relying more heavily on rhizoidal nutrient uptake (Larned 1998), potentially through exploiting the release of dissolved organic matter from scleractinian corals, thus reducing limitation otherwise encountered in sediments containing less organic material (Terrados & Ros 1991, Malta et al. 2005). This abundance is despite the nutrient-poor ambient conditions that make living in the northern bioregion of the Archipelago nearly impossible for other foliose algae (Tompkins & Wolff 2017). Therefore, unlike *Padina*, the thermal performance of *Caulerpa* is likely more contingent upon sediment composition than ambient nutrients alone. Thus, *Caulerpa* may experience less widespread, albeit patchier, locality-specific declines in abundance beyond its T_{opt} (28.8°C) due to its adaptive nutrient uptake strategy (Larned 1998, Malta et al. 2005).

Certain species, however, are predicted to benefit from warming and associated environmental change (Winder & Sommer 2012, Häder et al. 2014, Mangolte et al. 2022). For example, T_{opt} was highest for *Ulva* (i.e. by a minimum 5°C), and only E was significantly affected by enrichment. This may suggest that the alga is likely nutrient-saturated in its environment (Thomas et al. 2017, Bestion et al. 2018), with tissue concentrations too high for a notable shift in T_{opt}, and could favor some degree of warming. Additional studies in marine systems have similarly shown limited effects of nutrient additions on improving the growth and survival of primary producers at high temperatures (Franco et al. 2018, Fales et al. 2023), which, for some taxa, could suggest that temperatures beyond T_{opt} may accrue more physiological damage than stress from transient nutrient limitation (Mabin et al. 2013, Weigel et al. 2023). It could be that *Ulva* is more limited in productivity by high temperatures than low nutrient availability (potentially *Ochtodes*, too, although its much cooler T_{opt} likely reduces any perceived benefits of this tradeoff). However, whether its thermal tolerance and rapid rate of nutrient uptake (Steffensen 1976, Buapet et al. 2008, Teichberg et al. 2010) translate into increased abundance *in situ* appears to be context-specific (Karez et al. 2004, Kraufvelin 2007, Brandt et al. 2022) and may be dependent on additional ecological factors (Karez et al. 2004).

In low-latitude environments like the Galápagos Archipelago, heightened grazing pressure exerts a particularly strong influence (i.e. via top-down control) on benthic primary production, mainly as a function of the elevated metabolic rate of herbivores with temperature (Carr & Bruno 2013, Carr et al. 2018, Brandt et al. 2022). Studies here show overall declines in ephemeral biomass irrespective of nutrient availability or season, suggesting that algal abundance and distribution patterns may be more closely regulated by herbivory (Vinueza et al. 2006, Carr et al. 2018, Brandt et al. 2022). While *Ulva* has a T_{opt} likely well beyond that of its respective Galápagos grazing community, its capacity to remain at abundance levels high enough to ensure population persistence under the presence of ever-increasing herbivory is uncertain.

5. CONCLUSIONS

As ocean warming and its impacts on marine communities intensify, understanding the physiological responses of primary producers has become paramount. Our study elucidated the effects of nutrient—temperature interactions on the thermal performance of seaweeds in the Galápagos Archipelago, explicitly highlighting the context-dependency in genus-level responses to enrichment. This work provides insights into the future population dynamics of primary producers under continued warming: while some species may evidently experience declines in productivity — which may be heightened by nutrient stratification — the distribution and abundance of ephemeral taxa like *Ulva* with high thermal tolerance may be more closely regulated by additional ecological factors such as grazing. Changes to the structure of foundational primary producer communities are likely to simultaneously alter broader marine food web dynamics and higher-order interactions. These findings may be particularly relevant given the repeated onset of El Niño events in the Galápagos Archipelago, which not only elevate average temperatures but also imply periods of prolonged nutrient limitation.

Acknowledgements. We thank the Galápagos National Park Directorate for granting scientific investigation permit PC-27-22 to conduct this research and the Minister of Environment, Water and Ecological Transition for the genetic permit MAAE-DNB-CM-2021-0174 that allowed us to sequence the collected seaweed specimens. The Galapagos Science Center provided resource and facility provisioning (with special thanks to S. Sotamba, J. Sotamba, C. Vintimilla, and K. McKerr). Thanks to the University of North Carolina at Chapel Hill and partner institution Universidad San Francisco de Quito USFQ for their support of this study and associated students (S. A. Mantell, E. R. Srebnik, C. Parker, F. Rivera, N. De la Torre), who contributed both to field and laboratory-based data collection. This work was part of H.C.'s MSc thesis, available as a preprint at https://cdr.lib.unc.edu/concern/dissertations/x059ck071, and was funded by the National Science Foundation (OCE #2128592 to J.F.B. and M.B.).

LITERATURE CITED

Bennett S, Vaquer-Sunyer R, Jordá G, Forteza M and others (2022) Thermal performance of seaweeds and seagrasses across a regional climate gradient. Front Mar Sci 9: 733315

Best RJ, Stone MN, Stachowicz JJ (2015) Predicting consequences of climate change for ecosystem functioning: variation across trophic levels, species and individuals. Divers Distrib 21:1364–1374

Bestion E, Schaum C, Yvon-Durocher G (2018) Nutrient limitation constrains thermal tolerance in freshwater phytoplankton. Limnol Oceanogr Lett 3:436–443

Brandt M, Silva-Romero I, Fernández-Garnica D, Agudo-Adriani E and others (2022) Top-down and bottom-up control in the Galápagos upwelling system. Front Mar Sci 9:845635

Buapet P, Hiranpan R, Ritchie RJ, Prathep A (2008) Effect of nutrient inputs on growth, chlorophyll, and tissue nutrient concentration of *Ulva reticulata* from a tropical habitat. ScienceAsia 34:245–252

Capone HE (2023) Effects of nutrient availability on the thermal optima and sensitivities of Galápagos seaweeds. MS thesis, University of North Carolina at Chapel Hill, Chapel Hill, NC

Carr LA, Bruno JF (2013) Warming increases the top-down effects and metabolism of a subtidal herbivore. PeerJ 1: e109

Carr LA, Gittman RK, Bruno JF (2018) Temperature influences herbivory and algal biomass in the Galápagos Islands. Front Mar Sci 5:279

Ceccherelli G, Sechi N (2002) Nutrient availability in the sediment and the reciprocal effects between the native seagrass *Cymodocea nodosa* and the introduced rhizophytic alga *Caulerpa taxifolia.* Hydrobiologia 474:57–66

Chisholm JRM, Dauga C, Ageron E, Grimont PAD and others (1996) 'Roots' in mixotrophic algae. Nature 381: 382

Clausing RJ, Fong P (2016) Environmental variability drives rapid and dramatic changes in nutrient limitation of tropical macroalgae with different ecological strategies. Coral Reefs 35:669–680

Colvard N, Helmuth B (2017) Nutrients influence the thermal ecophysiology of an intertidal macroalga: Multiple stressors or multiple drivers? Ecol Appl 27:669–681

Delgado O, Rodríquez-Prieto C, Gacia E, Ballesteros E (1996) Lack of severe nutrient limitation in *Caulerpa taxifolia* (Vahl) C. Agardh, an introduced seaweed spreading over the oligotrophic northwestern Mediterranean. Bot Mar 39:61–67

Detmer AR, Miller RJ, Reed DC, Bell TW and others (2021) Variation in disturbance to a foundation species structures the dynamics of a benthic reef community. Ecology 102:e03304

Drohan A, Thoney D, Baker A (2005) Synergistic effect of high temperature and ultraviolet-B radiation on the gorgonian *Eunicea tourneforti* (Octocorallia: Alcyonacea: Plexauridae). Bull Mar Sci 77:257–266

Edgar GJ, Banks SA, Brandt M, Bustamante RH and others (2010) El Niño, grazers and fisheries interact to greatly elevate extinction risk for Galapagos marine species. Glob Change Biol 16:2876–2890

Eismann AI, Perpetuo Reis R, Ferreira da Silva A, Negrão Cavalcanti D (2020) *Ulva* spp. carotenoids: responses to environmental conditions. Algal Res 48:101916

Elser JJ, Bracken MES, Cleland EE, Gruner DS and others (2007) Global analysis of nitrogen and phosphorus limitation of primary producers in freshwater, marine and terrestrial ecosystems. Ecol Lett 10:1135–1142

Fales RJ, Weigel BL, Carrington E, Berry HD and others (2023) Interactive effects of temperature and nitrogen on the physiology of kelps (*Nereocystis luetkeana* and *Saccharina latissima*). Front Mar Sci 10:1281104

Fernández PA, Gaitán-Espitia JD, Leal PP, Schmid M and others (2020) Nitrogen sufficiency enhances thermal tolerance in habitat-forming kelp: implications for acclimation under thermal stress. Sci Rep 10:3186

Fong P, Boyer KE, Kamer K, Boyle KA (2003) Influence of initial tissue nutrient status of tropical marine algae on response to nitrogen and phosphorus additions. Mar Ecol Prog Ser 262:111–123

França FM, Benkwitt CE, Peralta G, Robinson JP and others (2020) Climatic and local stressor interactions threaten tropical forests and coral reefs. Philos Trans R Soc B 375: 20190116

Franco JN, Tuya F, Bertocci I, Rodríguez L and others (2018) The 'golden kelp' *Laminaria ochroleuca* under global change: integrating multiple eco-physiological responses with species distribution models. J Ecol 106:47–58

Freshwater DW, Rueness J (1994) Phylogenetic relationships of some European *Gelidium* (Gelidiales, Rhodophyta) species, based on *rbc*L nucleotide sequence analysis. Phycologia 33:187–194

Fu W, Randerson JT, Moore JK (2016) Climate change impacts on net primary production (NPP) and export production (EP) regulated by increasing stratification and phytoplankton community structure in the CMIP5 models. Biogeosciences 13:5151–5170

Gabrielson PW, Smith AC, Bruno JF, Vision TJ and others (2024) Taxonomic assessment of blade-forming *Ulva* species (Ulvales, Chlorophyta) in the Galápagos Archipelago, Ecuador using DNA sequencing. Bot Mar 67: 153–164

Gerard VA (1997) The role of nitrogen nutrition in high-temperature tolerance of the kelp, *Laminaria saccharina* (Chromophyta). J Phycol 33:800–810

Gissi E, Manea E, Mazaris AD, Fraschetti S and others (2021) A review of the combined effects of climate change and other local human stressors on the marine environment. Sci Total Environ 755:142564

Glynn PW, Feingold JS, Baker A, Banks S and others (2018) State of corals and coral reefs of the Galápagos Islands (Ecuador): past, present and future. Mar Pollut Bull 133: 717–733

Häder DP, Villafane VE, Helbling EW (2014) Productivity of aquatic primary producers under global climate change. Photochem Photobiol Sci 13:1370–1392

Hughey JR, Silva PC, Hommersand MH (2001) Solving taxonomic and nomenclatural problems in pacific Gigartinaceae (Rhodophyta) using DNA from type material. J Phycol 37:1091–1109

Jones PR (2019) A note on detecting statistical outliers in psychophysical data. Atten Percept Psychophys 81: 1189–1196

Karez R, Engelbert S, Kraufvelin P, Pedersen MF and others (2004) Biomass response and changes in composition of ephemeral macroalgal assemblages along an experimental gradient of nutrient enrichment. Aquat Bot 78: 103–117

Keith I, Bensted-Smith W, Banks S, Suarez J and others (2022) *Caulerpa chemnitzia* in Darwin threatening Galapagos coral reefs. PLOS ONE 17:e0272581

Komatsu T, Meinesz A, Buckles D (1997) Temperature and light responses of alga *Caulerpa taxifolia* introduced into the Mediterranean Sea. Mar Ecol Prog Ser 146:145–153

Kraufvelin P (2007) Responses to nutrient enrichment, wave action and disturbance in rocky shore communities. Aquat Bot 87:262–274

Larned ST (1998) Nitrogen-versus phosphorus-limited growth and sources of nutrients for coral reef macroalgae. Mar Biol 132:409–421

Larsson AI, Lundälv T, van Oevelen D (2013) Skeletal growth, respiration rate and fatty acid composition in the cold-water coral *Lophelia pertusa* under varying food conditions. Mar Ecol Prog Ser 483:169–184

Laufkötter C, Vogt M, Gruber N, Aita-Noguchi M and others (2015) Drivers and uncertainties of future global marine primary production in marine ecosystem models. Biogeosciences 12:6955–6984

Leys C, Ley C, Klein O, Bernard P and others (2013) Detecting outliers: do not use standard deviation around the mean, use absolute deviation around the median. J Exp Soc Psychol 49:764–766

Li G, Cheng L, Zhu J, Trenberth KE and others (2020) Increasing ocean stratification over the past half-century. Nat Clim Chang 10:1116–1123

Litchman E, Thomas MK (2023) Are we underestimating the ecological and evolutionary effects of warming? Interactions with other environmental drivers may increase species vulnerability to high temperatures. Oikos 2023: e09155

Littler MM, Littler DS, Titlyanov EA (1991) Comparisons of N- and P-limited productivity between high granitic islands versus low carbonate atolls in the Seychelles Archipelago: a test of the relative-dominance paradigm. Coral Reefs 10:199–209

Littler MM, Littler DS, Brooks BL (2006) Harmful algae on tropical coral reefs: bottom-up eutrophication and top-down herbivory. Harmful Algae 5:565–585

Mabin CJ, Gribben PE, Fischer A, Wright JT (2013) Variation in the morphology, reproduction and development of the habitat-forming kelp *Ecklonia radiata* with changing temperature and nutrients. Mar Ecol Prog Ser 483:117–131

Malta EJ, Ferreira DG, Vergara JJ, Pérez-Lloréns JL (2005) Nitrogen load and irradiance affect morphology, photosynthesis and growth of *Caulerpa prolifera* (Bryopsidales: Chlorophyta). Mar Ecol Prog Ser 298:101–114

Mangolte I, Lévy M, Dutkiewicz S, Clayton S and others (2022) Plankton community response to fronts: winners and losers. J Plankton Res 44:241–258

Marshall B, Biscoe PV (1980) A model for C_3 leaves describing the dependence of net photosynthesis on irradiance. J Exp Bot 31:29–39

Morikawa MK, Palumbi SR (2019) Using naturally occurring climate resilient corals to construct bleaching-resistant nurseries. Proc Natl Acad Sci USA 116:10586–10591

Nejrup LB, Staehr PA, Thomsen MS (2013) Temperature- and light-dependent growth and metabolism of the invasive red algae *Gracilaria vermiculophylla* — a comparison with two native macroalgae. Eur J Phycol 48:295–308

Olito C, White CR, Marshall DJ, Barneche DR (2017) Estimating monotonic rates from biological data using local linear regression. J Exp Biol 220:759–764

Ormaza-González F (2023) Cámara Nacional de Pesquería. https://camaradepesqueria.ec/la-nina-2020-2023-esta-terminando-nuevo-el-nino-en-gestacion/ (accessed 10 June 2024)

Padfield D, Matheson G (2018) nls.multstart: robust non-linear regression using AIC scores. R package version 1:1-5. https://CRAN.R-project.org/packages=nls.multstart

Padfield D, Yvon-Durocher G, Buckling A, Jennings S and others (2016) Rapid evolution of metabolic traits explains thermal adaptation in phytoplankton. Ecol Lett 19: 133–142

Padfield D, Lowe C, Buckling A, Ffrench-Constant R and others (2017) Metabolic compensation constrains the temperature dependence of gross primary production. Ecol Lett 20:1250–1260

Pedersen MF, Borum J (1996) Nutrient control of algal growth in estuarine waters. Nutrient limitation and the importance of nitrogen requirements and nitrogen storage among phytoplankton and species of macroalgae. Mar Ecol Prog Ser 142:261–272

R Core Team (2022) R: a language and environment for statistical computing. R Foundation for Statistical Computing, Vienna

Riegl B, Johnston M, Glynn PW, Keith I and others (2019) Some environmental and biological determinants of coral richness, resilience and reef building in Galápagos (Ecuador). Sci Rep 9:10322

Rousseeuw PJ, Croux C (1993) Alternatives to the median absolute deviation. J Am Stat Assoc 88:1273–1283

Russell BD, Thompson JAI, Falkenberg LJ, Connell SD (2009) Synergistic effects of climate change and local stressors: CO_2 and nutrient-driven change in subtidal rocky habitats. Glob Change Biol 15:2153–2162

Saunders GW, Kucera H (2010) An evaluation of *rbc*L, *tuf*A, UPA, LSU and ITS as DNA barcode markers for the marine green macroalgae. Cryptogam, Algol 31:487–528

Schaeffer B, Morrison J, Kamykowski D (2008) Phytoplankton biomass distribution and identification of productive habitats within the Galápagos Marine Reserve by MODIS, a surface acquisition system, and *in-situ* measurements. Remote Sens Environ 112:3044–3054

Schoolfield RM, Sharpe PJH, Magnuson CE (1981) Non-linear regression of biological temperature-dependent rate models based on absolute reaction-rate theory. J Theor Biol 88:719–731

Silbiger NJ, Goodbody-Gringley G, Bruno JF, Putnam HM (2019) Comparative thermal performance of the reef-building coral *Orbicella franksi* at its latitudinal range limits. Mar Biol 166:126

Silva-Romero I, Bruno JF, Silbiger NJ, Brandt M (2021) Local conditions influence thermal sensitivity of pencil urchin populations (*Eucidaris galapagensis*) in the Galápagos Archipelago. Mar Biol 168:34

Speare KE, Adam TC, Winslow EM, Lenihan HS and others (2022) Size-dependent mortality of corals during marine heatwave erodes recovery capacity of a coral reef. Glob Change Biol 28:1342–1358

Steffensen DA (1976) The effect of nutrient enrichment and temperature on the growth in culture of *Ulva lactuca* L. Aquat Bot 2:337–351

Takolander A, Leskinen E, Cabeza M (2017) Synergistic effects of extreme temperature and low salinity on foundational macroalga *Fucus vesiculosus* in the northern Baltic Sea. J Exp Mar Biol Ecol 495:110–118

Teichberg M, Fox SE, Olsen YS, Valiela I and others (2010) Eutrophication and macroalgal blooms in temperate and tropical coastal waters: nutrient enrichment experiments with *Ulva* spp. Glob Change Biol 16:2624–2637

Terrados J, Ros J (1991) Production dynamics in a macrophyte-dominated ecosystem: the Mar Menor coastal lagoon (SE Spain). Oecol Aquat 10:255–270

Thomas MK, Aranguren-Gassis M, Kremer CT, Gould MR and others (2017) Temperature nutrient interactions exacerbate sensitivity to warming in phytoplankton. Glob Change Biol 23:3269–3280

Thomson JA, Burkholder DA, Heithaus MR, Fourqurean JW and others (2015) Extreme temperatures, foundation species, and abrupt ecosystem change: an example from an iconic seagrass ecosystem. Glob Change Biol 21: 1463–1474

Tompkins P, Wolff M (2017) Galápagos macroalgae: a review of the state of ecological knowledge. Rev Biol Trop 65: 375–392

Van de Waal DB, Litchman E (2020) Multiple global change stressor effects on phytoplankton nutrient acquisition in a future ocean. Philos Trans R Soc B 375: 20190706

Vermeij MJ, van Moorselaar I, Engelhard S, Hörnlein C and others (2010) The effects of nutrient enrichment and herbivore abundance on the ability of turf algae to overgrow coral in the Caribbean. PLOS ONE 5:e14312

Vinueza LR, Branch GM, Branch ML, Bustamante RH (2006) Top-down herbivory and bottom-up El Niño effects on Galápagos rocky-shore communities. Ecol Monogr 76: 111–131

Voolstra CR, Buitrago-López C, Perna G, Cárdenas A and others (2020) Standardized short-term acute heat stress assays resolve historical differences in coral thermotolerance across microhabitat reef sites. Glob Change Biol 26: 4328–4343

Weigel BL, Small SL, Berry HD, Dethier MN (2023) Effects of temperature and nutrients on microscopic stages of the bull kelp (*Nereocystis luetkeana*, Phaeophyceae). J Phycol 59:893–907

Wernberg T, de Bettignies T, Joy BA, Finnegan PM (2016) Physiological responses of habitat-forming seaweeds to increasing temperatures. Limnol Oceanogr 61:2180–2190

Williams SL (1984) Uptake of sediment ammonium and translocation in a green macroalga *Caulerpa cupressiodes.* Limnol Oceanogr 29:374–379

Williams SL, Breda VA, Anderson TW, Nyden BB (1985) Growth and sediment disturbances of *Caulerpa* spp. (Chlorophyta) in a submarine canyon. Mar Ecol Prog Ser 21:275–281

Winder M, Sommer U (2012) Phytoplankton response to a changing climate. Hydrobiologia 698:5–16

Wolff NH, Mumby PJ, Devlin M, Anthony KR (2018) Vulnerability of the Great Barrier Reef to climate change and local pressures. Glob Change Biol 24:1978–1991

Appendix.

Table A1. List of sequenced specimens used in thermal tolerance experiments, each with its herbarium accession number, collection data, and GenBank accession number. Specific epithets in single quotes indicate specimens not linked to type material; (—) sequence not obtained

Species	Herbarium accession no.	Collection data	GenBank accession no. *rbc*L	*tuf*A
Caulerpa '*racemosa*'	NCU 683287	Bahía Rosa Blanca (San Cristóbal Island), Galápagos Archipelago, Ecuador, 21.xi.2022, sand bottom bay (1–2 m depths), *leg.* H. Capone & N. Chico	—	PP841602
Caulerpa '*racemosa*'	NCU 683288	Bahía Rosa Blanca (San Cristóbal Island), Galápagos Archipelago, Ecuador, 23.xi.2022, sand bottom bay (1–2 m depths), *leg.* H. Capone & N. Chico	—	PP841603
Caulerpa '*racemosa*'	NCU 683289	Bahía Rosa Blanca (San Cristóbal Island), Galápagos Archipelago, Ecuador, 22.xi.2022, sand bottom bay (1–2 m depths), *leg.* H. Capone & N. Chico	—	PP841604
Caulerpa '*racemosa*'	NCU 683290	Bahía Rosa Blanca (San Cristóbal Island), Galápagos Archipelago, Ecuador, 23.xi.2022, sand bottom bay (1–2 m depths), *leg.* H. Capone & N. Chico	—	PP841605
Ochtodes	NCU 683291	Punta Carola (San Cristóbal Island), Galápagos Archipelago, Ecuador, 20.xi.2022, rocky subtidal (1–2 m depths), *leg.* H. Capone & E. Agudo	PP841606	—
Ochtodes	NCU 683292	Punta Carola (San Cristóbal Island), Galápagos Archipelago, Ecuador, 20.xi.2022, rocky subtidal (1–2 m depths), *leg.* H. Capone & E. Agudo	PP841607	—
Ochtodes	NCU 683293	Punta Carola (San Cristóbal Island), Galápagos Archipelago, Ecuador, 12.xi.2022, rocky subtidal (1–2 m depths), *leg.* C. Parker & E. R. Srebnik	PP841608	—
Ochtodes	NCU 683294	Punta Carola (San Cristóbal Island), Galápagos Archipelago, Ecuador, 12.xi.2022, rocky subtidal (1–2 m depths), *leg.* C. Parker & E. R. Srebnik	PP841609	—
Ulva ohnoi	NCU 683295	Punta Carola (San Cristóbal Island), Galápagos Archipelago, Ecuador, 11.xi.2022, rocky subtidal (≤1 m depths), *leg.* F. Rivera & N. de la Torre	PP841610	PP841611
Ulva ohnoi	NCU 683296	Punta Carola (San Cristóbal Island), Galápagos Archipelago, Ecuador, 11.xi.2022, rocky subtidal (≤1 m depths), *leg.* F. Rivera & N. de la Torre	—	PP841612
Ulva ohnoi	NCU 683297	Punta Carola (San Cristóbal Island), Galápagos Archipelago, Ecuador, 18.xi.2022, rocky subtidal (≤1 m depths), *leg.* H. Capone & F. Rivera	PP841613	—
Ulva lactuca	NCU 683298	Punta Carola (San Cristóbal Island), Galápagos Archipelago, Ecuador, 18.xi.2022, rocky subtidal (≤1 m depths), *leg.* H. Capone & F. Rivera	PP841615	PP841616
Ulva ohnoi	NCU 683299	Punta Carola (San Cristóbal Island), Galápagos Archipelago, Ecuador, 14.xi.2022, rocky subtidal (≤1 m depths), *leg.* C. Parker & E. R. Srebnik	PP841614	—

Editorial responsibility: John N. Griffin,
Swansea, UK
Reviewed by: C. R. Fong and 2 anonymous referees

Submitted: February 29, 2024
Accepted: October 2, 2024
Proofs received from author(s): November 18, 2024